

LOCAL BUCKLING OF THIN-WALLED CIRCULAR HOLLOW SECTION UNDER UNIFORM BENDING

Bui Hung Cuong^{a,*}

^a*Faculty of Building and Industrial Construction, Hanoi University of Civil Engineering,
55 Giai Phong road, Hai Ba Trung district, Hanoi, Vietnam*

Article history:

Received 08/06/2021, Revised 01/7/2021, Accepted 12/7/2021

Abstract

This article presents a semi-analytical finite strip method based on Marguerre's shallow shell theory and Kirchhoff's assumption. The formulated finite strip is used to study the buckling behavior of thin-walled circular hollow sections (CHS) subjected to uniform bending. The shallow finite strip program of the present study is compared to the plate strip implemented in CUFSM4.05 program for demonstrating the accuracy and better convergence of the former. By varying the length of the CHS, the signature curve relating buckling stresses to half-wave lengths is established. The minimum local buckling point with critical stress and corresponding critical length can be found from the curve. Parametric studies are performed to propose approximative expressions for calculating the local critical stress and local critical length of steel and aluminium CHS.

Keywords: circular hollow section; finite strip; local buckling; signature curve; shallow shell theory.

[https://doi.org/10.31814/stce.huce\(nuce\)2021-15\(4\)-08](https://doi.org/10.31814/stce.huce(nuce)2021-15(4)-08) © 2021 Hanoi University of Civil Engineering (HUCE)

1. Introduction

The semi-analytical finite strip method (SAFSM) pioneered by Cheung [1] is a derivative of the finite element method. In plated structural members, the SAFSM uses trigonometric functions in the longitudinal direction and polynomial functions in the transversal direction. Thus, this method can be considered as an application of Fourier series in the analysis of structures. Because selected trigonometric functions must satisfy boundary conditions, the SAFSM is convenient to analyze members which have two ends such as: simple-simple, clamped-clamped, simple-clamped, clamped-free, clamped-guided [2–5]. An outstanding application of the SAFSM is the buckling analysis of thin-walled members. When the local buckling is in the consideration, thin walls of the member are buckled by numerous half-wave length in the longitudinal direction. The boundary conditions have very little influence on the local buckling. Therefore, sinusoidal functions which satisfy simply supported members are extensively used in the literature [6–11]. The SAFSM reduces greatly simulation and computation time in the analysis of thin-walled members because a few strips are used for modelling the cross section of the member, and the mathematical manipulation is analytically realized in the longitudinal direction. Thus, 3D problems are reduced to 2D ones. An interesting presentation of the SAFSM in the buckling analysis is the signature curve which relates buckling stresses to half-wave lengths [12]. From this curve, the local and distortional buckling are simply detected by local minimums. Most of finite strips were developed based on the Kirchhoff or Mindlin plate theories except

*Corresponding author. *E-mail address:* bhungcuong@gmail.com (Cuong, B. H.)

the shallow strip in [13] formulated on Marguerre’s shallow shell theory [14]. The shallow strip was used to investigate the buckling behavior of cold-formed sections with curved corners, this strip is not used to analyze circular hollow sections (CHS) yet.

CHS is widely used in civil and industrial engineering such as: columns, tubular piles, tubular members of truss, tanks, pipelines, electric poles, wind turbines, . . . When the ratio of diameter to thickness is high, CHS is susceptible to be locally buckled. The traditional design against the local buckling of CHS follows two steps: first, the critical stress is determined by a linear buckling analysis then an empirical factor is applied to account the discrepancy between linear critical stress and experimental results. This approach has shown a satisfaction in the practice design [15]. Therefore, the study on the linear buckling of CHS is necessary [16–18]. Due to the gradient stress distributed on the cross section, there are not explicit analytical expressions for calculating the local critical stress of the CHS subjected to uniform bending. Instead, the local critical stress of CHS under uniform bending can be approximatively determined by the formula of the local critical stress of CHS under axial compression as advised by [15, 16, 19].

The present work poses to study the buckling behavior of thin-walled circular hollow sections (CHS) under uniform bending by the SAFSM. The finite strip is formulated from the shallow shell theory of Marguerre [13, 14] and Kirchhoff’s assumption. The exactness and the convergence of the shallow finite strip is proved when comparing to the plate finite strip implemented in CUFSM 4.05 program [20]. The shallow finite strip is used to numerically analyze CHS when the length is varied. From that, the signature curve of CHS is obtained. The local buckling of CHS subjected to uniform bending can be detected from the curve, the results are critical stress and critical length. Numerous steel and aluminium CHS with the ratio between thickness and radius varying are analyzed to proposed approximative expressions for the determination of local critical stress and local critical length. Small coefficient of variation and high coefficients of determination validate the proposed expressions.

2. Formulation of finite strip

Fig. 1 draws a cylindrical 3 nodal-line finite strip which is formulated from Marguerre’s shallow shell theory [13, 14] and Kirchhoff’s assumption. The relation between strains and displacements is written as:

$$\epsilon_x = \frac{\partial u}{\partial x} - z \frac{\partial^2 w}{\partial x^2} + \frac{\partial h}{\partial x} \frac{\partial w}{\partial x} \tag{1}$$

$$\epsilon_y = \frac{\partial v}{\partial y} - z \frac{\partial^2 w}{\partial y^2} + \frac{\partial h}{\partial y} \frac{\partial w}{\partial y} \tag{2}$$

$$\gamma_{xy} = \frac{\partial u}{\partial y} + \frac{\partial v}{\partial x} - 2z \frac{\partial^2 w}{\partial x \partial y} + \frac{\partial h}{\partial x} \frac{\partial w}{\partial y} + \frac{\partial h}{\partial y} \frac{\partial w}{\partial x} \tag{3}$$

Rotations are calculated from the out-of-plane translation:

$$\theta_x = \frac{\partial w}{\partial y} \tag{4}$$

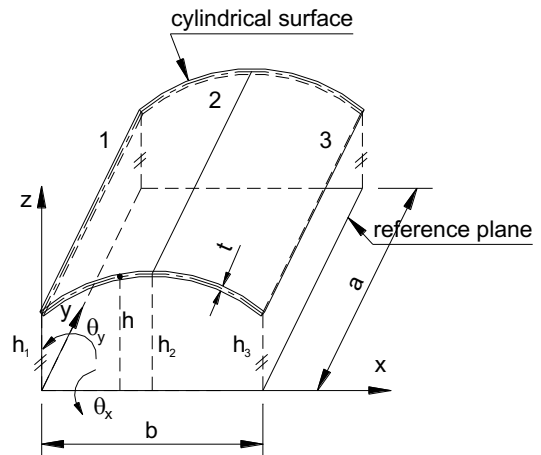


Figure 1. Shallow shell finite strip with 3-nodal line

$$\theta_y = \frac{\partial w}{\partial x} \tag{5}$$

where u, v , and w are translations w.r.t x, y and z directions in the Cartesian coordinates of the reference plane; θ_x and θ_y are rotations about x and y axis; h is the distance from a point in the curved middle surface to the reference plane.

Noted that in the shallow shell of Marguerre, the manipulation is realized on the reference plane instead of the curved surface.

Three translations u, v , and w of simply supported finite strip can be expressed by series of sinusoidal functions in the longitudinal direction and polynomial functions in the transversal direction [1] below:

$$u(x, y) = \sum_{m=1}^r \left\{ \begin{matrix} H_1 & H_2 & H_3 \end{matrix} \right\} \left\{ \begin{matrix} u_{1m} \\ u_{2m} \\ u_{3m} \end{matrix} \right\} \sin \frac{m\pi y}{a} \tag{6}$$

$$v(x, y) = \sum_{m=1}^r \left\{ \begin{matrix} H_1 & H_2 & H_3 \end{matrix} \right\} \left\{ \begin{matrix} v_{1m} \\ v_{2m} \\ v_{3m} \end{matrix} \right\} \cos \frac{m\pi y}{a} \tag{7}$$

$$w(x, y) = \sum_{m=1}^r \left\{ \begin{matrix} H_{w1} & H_{\theta1} & H_{w2} & H_{\theta2} & H_{w3} & H_{\theta3} \end{matrix} \right\} \left\{ \begin{matrix} w_{1m} \\ \theta_{1m} \\ w_{2m} \\ \theta_{2m} \\ w_{3m} \\ \theta_{3m} \end{matrix} \right\} \sin \frac{m\pi y}{a} \tag{8}$$

in which:

$$H_1 = 1 - \frac{3x}{b} + \frac{2x^2}{b^2}; \quad H_2 = \frac{4x}{b} - \frac{4x^2}{b^2}; \quad H_3 = -\frac{x}{b} + \frac{2x^2}{b^2} \tag{9}$$

$$H_{w1} = 1 - \frac{23x^2}{b^2} + \frac{66x^3}{b^3} - \frac{68x^4}{b^4} + \frac{24x^5}{b^5}; \quad H_{\theta1} = x - \frac{6x^2}{b} + \frac{13x^3}{b^2} - \frac{12x^4}{b^3} + \frac{4x^5}{b^4} \tag{10}$$

$$H_{w2} = \frac{16x^2}{b^2} - \frac{32x^3}{b^3} + \frac{16x^4}{b^4}; \quad H_{\theta2} = -\frac{8x^2}{b} + \frac{32x^3}{b^2} - \frac{40x^4}{b^3} + \frac{16x^5}{b^4} \tag{11}$$

$$H_{w3} = \frac{7x^2}{b^2} - \frac{34x^3}{b^3} + \frac{52x^4}{b^4} - \frac{24x^5}{b^5}; \quad H_{\theta3} = -\frac{x^2}{b} + \frac{5x^3}{b^2} - \frac{8x^4}{b^3} + \frac{4x^5}{b^4} \tag{12}$$

The distance from a point in the curved middle surface to the reference plane, h in Eqs. (1)–(3) is interpolated as:

$$h(x, y) = \left\{ \begin{matrix} H_1 & H_2 & H_3 \end{matrix} \right\} \left\{ \begin{matrix} h_1 \\ h_2 \\ h_3 \end{matrix} \right\}.1 \tag{13}$$

The stiffness matrix of a finite strip in the local axes can be obtained from the strain energy.

$$U = \frac{1}{2} \int_{-t/2}^{t/2} \int_A \{\varepsilon\}^T [D] \{\varepsilon\} dAdz \tag{14}$$

in which A is the area of the reference plane of the curved strip. $\{\varepsilon\}$ are strains determined by Eqs. (1)÷(3)

$$\{\varepsilon\} = \left\{ \varepsilon_x \quad \varepsilon_y \quad \gamma_{xy} \right\} \quad (15)$$

$[D]$ is the matrix of elasticity.

$$[D] = \begin{bmatrix} \frac{E}{1-\nu^2} & \frac{\nu E}{1-\nu^2} & 0 \\ \frac{\nu E}{1-\nu^2} & \frac{E}{1-\nu^2} & 0 \\ 0 & 0 & G \end{bmatrix} \quad (16)$$

Replacing Eqs. (6)÷(8) and (13) into Eqs. (1)÷(3), the strains can be obtained as following:

$$\{\varepsilon\} = \sum_{m=1}^r [B_m] \{\delta_m\} = \sum_{m=1}^r \left[\begin{array}{ccc} B_{1m} & B_{2m} & B_{3m} \end{array} \right] \left\{ \delta_{1m} \quad \delta_{2m} \quad \delta_{3m} \right\}^T \quad (17)$$

where for nodal line i and m^{th} harmonic, typical term has the form:

$$[B_{im}] = \begin{bmatrix} \frac{dH_i}{dx} s_m & 0 & -z \frac{d^2 H_{wi}}{dx^2} s_m + \frac{dh}{dx} \frac{dH_{wi}}{dx} s_m & -z \frac{d^2 H_{\theta i}}{dx^2} s_m + \frac{dh}{dx} \frac{dH_{\theta i}}{dx} s_m \\ 0 & -H_i k_m s_m & z H_{wi} k_m^2 s_m & z H_{\theta i} k_m^2 s_m \\ H_i k_m c_m & \frac{dH_i}{dx} c_m & -2z \frac{dH_{wi}}{dx} k_m c_m + \frac{dh}{dx} H_{wi} k_m c_m & -2z \frac{dH_{\theta i}}{dx} k_m c_m + \frac{dh}{dx} H_{\theta i} k_m c_m \end{bmatrix} \quad (18)$$

$$\{\delta_{im}\} = \left\{ u_{im} \quad v_{im} \quad w_{im} \quad \theta_{im} \right\}^T \quad (19)$$

with

$$k_m = \frac{m\pi}{a}; \quad s_m = \sin(k_m y); \quad c_m = \cos(k_m y) \quad (20)$$

Replacing Eq. (17) into Eq. (14) to get the stiffness matrix of the shallow strip.

$$[K]_e = \begin{bmatrix} [K_{11}]_e & 0 & \dots & 0 \\ 0 & [K_{22}]_e & \dots & 0 \\ \dots & \dots & \dots & \dots \\ 0 & 0 & \dots & [K_{rr}]_e \end{bmatrix} \quad (21)$$

where

$$[K_{mm}]_e = \int_{-t/2}^{t/2} \int_0^a \int_0^b \int_A [B_m]^T [D] [B_m] dx dy dz \quad (22)$$

Noted that for the simply supported finite strip, sinusoidal terms are uncoupled. Therefore, the stiffness matrix has a diagonal form as indicated in Eq. (21).

In the linear elastic buckling analysis, the geometric matrix can be determined from the potential energy done by initial membrane stresses $\{\sigma_o\}$ on nonlinear membrane strains $\{\varepsilon_{NL}\}$ [11].

$$W = \frac{1}{2} \int_A 2 \{\sigma_o\} \{\varepsilon_{NL}\} t dA \quad (23)$$

where

$$\{\sigma_o\} = \left\{ \sigma_{ox} \quad \sigma_{oy} \quad \tau_{oxy} \right\} \quad (24)$$

$$\{\varepsilon_{NL}\} = \left\{ \varepsilon_{NLx} \quad \varepsilon_{NLy} \quad \gamma_{NLxy} \right\}^T \quad (25)$$

The nonlinear strains are determined from nonlinear parts of Green's deformations:

$$\varepsilon_{NLx} = \frac{1}{2} \left[\left(\frac{\partial u}{\partial x} \right)^2 + \left(\frac{\partial v}{\partial x} \right)^2 + \left(\frac{\partial w}{\partial x} \right)^2 \right] \quad (26)$$

$$\varepsilon_{NLy} = \frac{1}{2} \left[\left(\frac{\partial u}{\partial y} \right)^2 + \left(\frac{\partial v}{\partial y} \right)^2 + \left(\frac{\partial w}{\partial y} \right)^2 \right] \quad (27)$$

$$\gamma_{NLxy} = \left(\frac{\partial u}{\partial x} \frac{\partial u}{\partial y} + \frac{\partial v}{\partial x} \frac{\partial v}{\partial y} + \frac{\partial w}{\partial x} \frac{\partial w}{\partial y} \right) \quad (28)$$

In the present work, only longitudinal initial stress σ_{oy} , and longitudinal nonlinear strain ε_{NLy} are considered as presented in [13]. The longitudinal initial stress can be seen as linearly distributed in the transversal direction within a strip (Fig. 2).

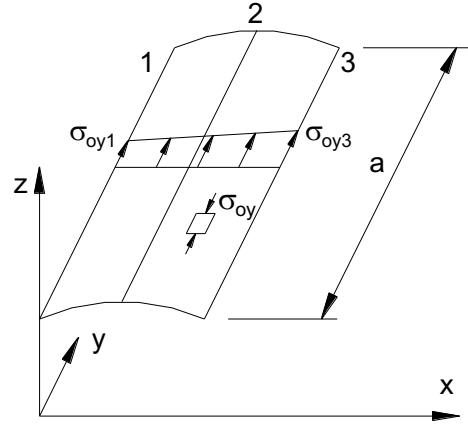


Figure 2. Linear distributed of longitudinal initial stress

$$\sigma_{oy} = \sigma_{oy1} - (\sigma_{oy1} - \sigma_{oy3}) \frac{x}{b} \quad (29)$$

Hence, the potential energy (Eq. (23)) can be rewritten:

$$W = \frac{1}{2} \int_A \left[\sigma_{oy1} - (\sigma_{oy1} - \sigma_{oy3}) \frac{x}{b} \right] \left[\left(\frac{\partial u}{\partial y} \right)^2 + \left(\frac{\partial v}{\partial y} \right)^2 + \left(\frac{\partial w}{\partial y} \right)^2 \right] t dA \quad (30)$$

The geometric matrix can be determined when the Eqs. (6)–(8) are substituted into Eq. (30). It is noted that for simply supported finite strip, harmonic terms are uncoupled, thus the geometric matrix has a diagonal form [1]:

$$[K_G]_e = \begin{bmatrix} [K_{G11}]_e & 0 & \dots & 0 \\ 0 & [K_{G22}]_e & \dots & 0 \\ \dots & \dots & \dots & \dots \\ 0 & 0 & \dots & [K_{Grr}]_e \end{bmatrix} \quad (31)$$

The eigenequation is used for the linear elastic buckling analysis:

$$([K] + \lambda [K_G]) \{\delta\} = 0 \quad (32)$$

in which the eigenvalue λ giving buckling load and the corresponding eigenvector $\{\delta\}$ related to the buckling shape of the structure. $[K]$ and $[K_G]$ are stiffness matrix and geometric matrix of the structure in global axes. The global stiffness matrix and geometric matrix of the structure are given by the summation of local ones which are transferred from the local axes into the global axes. Despite the presentation of multiple series in the longitudinal direction (Eq. (6)–(8)), but in practice, the use of the first harmonic term, $m = 1$ is sufficient for the linear elastic analysis.

3. Validation and parametric studies

To validate the shallow shell finite strip formulated in the previous section, firstly the convergent study is performed and compared to a result calculated by Sylvestre [17], and CUFSM4.05 program [20] in which the finite strip based on Kirchhoff's plate theory is implemented. As follows, a steel CHS with radius of 50 mm and thickness of 1 mm is analyzed, the modulus of elasticity and Poisson ratio are 210000 N/mm² and 0.3, respectively. Sylvestre [17] who utilized the Generalized Beam Theory (GBT) provided numerically the local critical stress with the value of 2590 N/mm², this critical stress corresponds to a critical length, 13 mm of CHS. Respectively, 24, 48, 60, 96, 120, 160, and 200 nodal lines are used to model the CHS by the shallow strip of the present work and plate strip of CUFSM4.05 program. The convergent results are depicted in Fig. 3. Both plate strip and shallow strip approach to a value very little higher than Sylvestre's critical stress (plate strip – 2604 N/mm², shallow strip – 2597 N/mm², both with 200 nodal lines). But the shallow strip gives a better convergence because even using 60 nodal lines (30 shallow strips), the result is already 2601 N/mm².

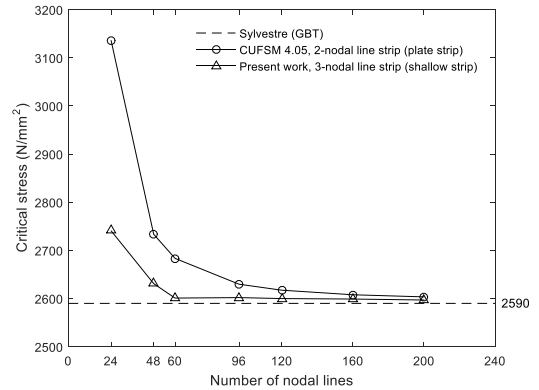


Figure 3. Convergent study

The above results are obtained when only the first harmonic term, $m = 1$ in Eqs. (6)–(8) is used. The buckling shape corresponding to the local critical stress and local critical length drawn by the shallow strip program is presented in Fig. 4(a). Figs. 4(b, c) depict two other buckling shapes with the same local critical stress but different harmonic terms, i.e., $m = 5$ and $m = 50$. That is, a longer CHS is locally buckled with numerous half-waves, each half-wave is equal to the local critical length. Thus, the use of the first harmonic term is sufficient to study the buckling behavior of CHS. Another comment that can be deduced is the long CHS of different boundary conditions being locally buckled with the same critical stress of the simply supported one because of long distances, the boundary conditions at two ends of CHS influence very little on the local buckling.

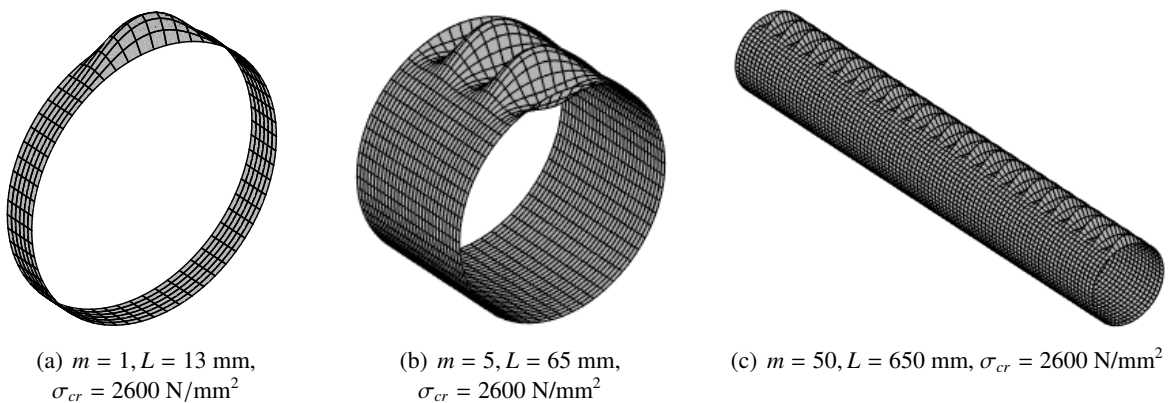


Figure 4. Buckling shapes modelled by 60 shallow strips (120 nodal lines)

Secondly, for better understanding the buckling behavior of the above CHS, the signature curve is established. This curve can be easily provided by FSM when the length of the CHS varies. Noted that the first harmonic term is always used. Fig. 5 shows signature curves when the CHS is modeled by 60, 96, and 120 nodal lines of the shallow strip program and by 200 nodal lines by CUFSM 4.05 program. All signature curves can detect the unique local buckling of the CHS. But after the local buckling point, the modeling by 60 nodal lines (or 30 shallow finite strips) gives stiffer solutions. While the rest give a very good fit each other. Henceforth, the modeling of CHS with 60 shallow strips (120 nodal lines) will be used.

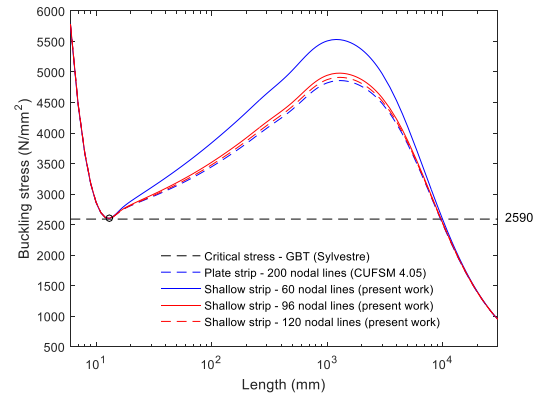


Figure 5. Signature curves buckling stress – length of CHS 50×1mm

The local buckling shape was depicted in Fig. 4. Fig. 6 draws other buckling shapes corresponding to longer lengths of CHS.

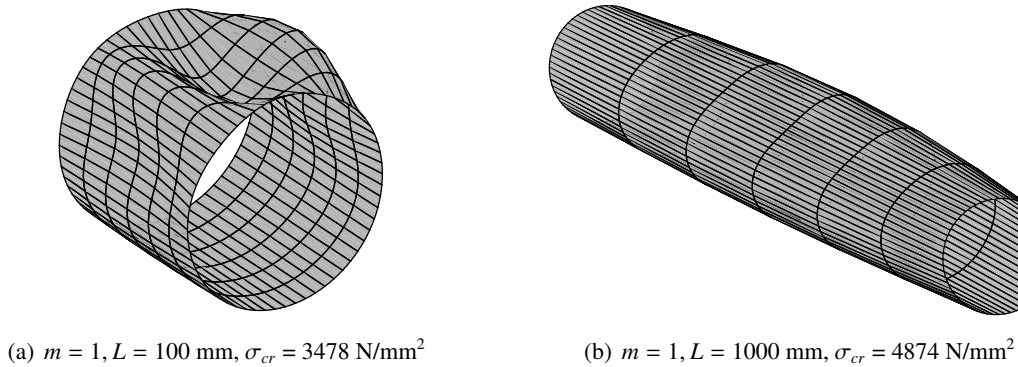


Figure 6. Buckling shapes of longer CHS modeled by 60 shallow strips (120 nodal lines)

Thirdly, the research about the dependence of the local buckling on thickness to radius and length to radius ratios is performed. Due to the gradient stress distributed on the cross section of CHS, there are not explicit analytical expressions for the local critical stress and local critical length of CHS subjected to uniform bending. Therefore, the formulas established for CHS under uniform compression are instead mentioned in safety side as advised by [16, 19]. The local critical stress of CHS under uniform compression can be obtained from the formula following:

$$\sigma_{cr,c} = \frac{E}{\sqrt{3(1-\nu^2)}} \frac{t}{R} \tag{33}$$

This local critical stress corresponds to the local critical length given by:

$$L_{cr,c} = \pi \sqrt[4]{\frac{R^2 t^2}{12(1-\nu^2)}} \tag{34}$$

Dividing Eq. (34) by R :

$$\frac{L_{cr,c}}{R} = \pi \sqrt[4]{\frac{1}{12(1-\nu^2)} \left(\frac{t}{R}\right)^2} \quad (35)$$

From Eqs. (33), (35), it can be found that the local critical stress depends on t/R and L/R ratios. In other words, local critical stresses are equals for two CHS of the same t/R and L/R ratios. One can guess the local critical stress of CHS subjected to uniform bending depending also on t/R and L/R ratios. The shallow finite strip program can numerically demonstrate this guess. Three thickness to radius ratios are in the consideration, namely $t/R = 1/25, 1/50, \text{ and } 1/100$. Two steel CHS are analyzed for each t/R ratio. Signature curves relating buckling stress to L/R ratio are provided in Fig. 7. The signature curves of steel CHS with same t/R ratio coincide totally not only at the local critical point but at other buckling points.

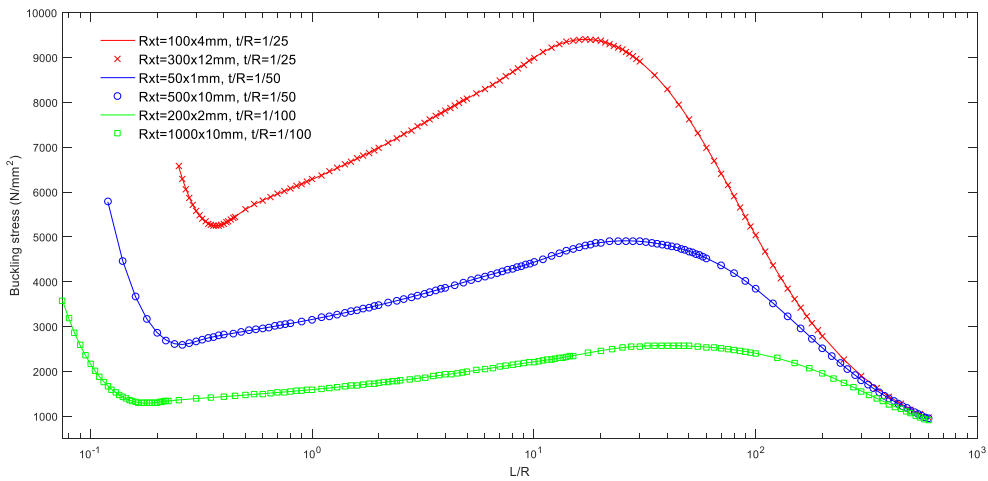


Figure 7. Signature curves buckling stress – L/R ratio of CHS

Finally, from the above research, expressions for determining the local critical length, $L_{cr,b}$ and local critical stress, $\sigma_{cr,b}$ of steel CHS and aluminium CHS under uniform bending can be proposed by parametric studies.

About the local critical length, Tables 1 and 2 present parametric studies for steel CHS and aluminium CHS. The t/R ratios are chosen so that CHS is considered thin-walled. The ratio of $L_{cr,b}$ to $L_{cr,c}$ is calculated, in which $L_{cr,c}$ is determined from Eq. (34).

It can be found from Tables 1 and 2 that with each t/R ratio, the values of $L_{cr,b}/L_{cr,c}$ are almost the same for steel CHS and aluminium CHS. Therefore, an approximative expression can be commonly proposed for CHS under uniform bending:

$$L_{cr,b} = \left[-21.376 \left(\frac{t}{R}\right)^2 + 2.1567 \left(\frac{t}{R}\right) + 1.0152 \right] \pi \sqrt[4]{\frac{R^2 t^2}{12(1-\nu^2)}} \quad (36)$$

Table 1. Parametric study of local critical length for steel CHS: $E = 2.1 \times 10^5 \text{ N/mm}^2$, $\nu = 0.3$

t/R	$L_{cr,b}/L_{cr,c}$ numerical analysis	$L_{cr,b}/L_{cr,c}$ Eq. (36)
1/20	1.0713	1.0696
1/25	1.0647	1.0673
1/50	1.0474	1.0498
1/75	1.0423	1.0402
1/100	1.0358	1.0346
1/150	1.0325	1.0286
1/200	1.0270	1.0254
1/300	1.0223	1.0222
1/400	1.0184	1.0205
1/500	1.0157	1.0194
CV: 0.0024		
R^2 : 0.9823		

Table 2. Parametric study of local critical length for aluminium CHS: $E = 0.7 \times 10^5 \text{ N/mm}^2$, $\nu = 0.33$

t/R	$L_{cr,b}/L_{cr,c}$ numerical analysis	$L_{cr,b}/L_{cr,c}$ Eq. (36)
1/20	1.0747	1.0696
1/25	1.0649	1.0673
1/50	1.0501	1.0498
1/75	1.0435	1.0402
1/100	1.0361	1.0346
1/150	1.0316	1.0286
1/200	1.0277	1.0254
1/300	1.0219	1.0222
1/400	1.0188	1.0205
1/500	1.0155	1.0194
CV: 0.0028		
R^2 : 0.9781		

About the local critical stress, Tables 3 and 4 show parametric studies for steel CHS and aluminium CHS. The ratio of $\sigma_{cr,b}$ to $\sigma_{cr,c}$ is calculated, in which $\sigma_{cr,c}$ is determined from Eq. (33).

It can be found from Tables 3 and 4 that with each t/R ratio, the values of $\sigma_{cr,b}/\sigma_{cr,c}$ are almost the same for steel CHS and aluminium CHS. Therefore, an approximative expression of the critical stress can be commonly proposed for CHS under uniform bending:

$$\sigma_{cr,b} = \left[-7.1619 \left(\frac{t}{R} \right)^2 + 0.9402 \left(\frac{t}{R} \right) + 1.0065 \right] \frac{E}{\sqrt{3(1-\nu^2)}} \frac{t}{R} \quad (37)$$

Table 3. Parametric study of local critical stress for steel CHS: $E = 2.1 \times 10^5 \text{ N/mm}^2$, $\nu = 0.3$

t/R	$\sigma_{cr,b}/\sigma_{cr,c}$ numerical analysis	$\sigma_{cr,b}/\sigma_{cr,c}$ Eq. (37)
1/20	1.0359	1.0356
1/25	1.0322	1.0326
1/50	1.0224	1.0224
1/75	1.0180	1.0178
1/100	1.0155	1.0152
1/150	1.0126	1.0124
1/200	1.0111	1.0110
1/300	1.0094	1.0096
1/400	1.0087	1.0088
1/500	1.0082	1.0084
CV: 0.00024		
R^2 : 0.9994		

Table 4. Parametric study of local critical stress for aluminium CHS: $E = 0.7 \times 10^5 \text{ N/mm}^2$, $\nu = 0.33$

t/R	$\sigma_{cr,b}/\sigma_{cr,c}$ numerical analysis	$\sigma_{cr,b}/\sigma_{cr,c}$ Eq. (37)
1/20	1.0358	1.0356
1/25	1.0321	1.0326
1/50	1.0224	1.0224
1/75	1.0181	1.0178
1/100	1.0155	1.0152
1/150	1.0127	1.0124
1/200	1.0111	1.0110
1/300	1.0095	1.0096
1/400	1.0087	1.0088
1/500	1.0082	1.0084
CV: 0.00027		
R^2 : 0.9992		

4. Conclusions

A 3-nodal lines finite strip based on Marguerre's shallow shell theory and Kirchhoff's assumption is formulated and proves a better convergence than the plate finite strip. This shallow finite strip is efficient in the linear buckling analysis of circular hollow section. The signature curve detects a unique local buckling point of CHS subjected under uniform bending. Numerical solutions show the dependence of the local critical stress on thickness to radius and length to radius ratios. Through parametric studies performed by the shallow finite strip program, two approximative expressions for determining the local critical length and local critical stress are proposed. These expressions can provide more accurate values of the local buckling of CHS under uniform bending than the usual advice of using the classical solution of axially compressed CHS.

References

- [1] Cheung, Y. K. (1976). [Finite strip method](#). In *Finite Strip Method in Structural Analysis*, Elsevier, 1–24.
- [2] Bradford, M. A., Azhari, M. (1995). [Buckling of plates with different end conditions using the finite strip method](#). *Computers & Structures*, 56(1):75–83.
- [3] Li, Z. (2011). *Finite strip modeling of thin-walled members*. Ph. D dissertation, Johns Hopkins University, Baltimore, USA.
- [4] Li, Z., Schafer, B. W. (2013). [Constrained Finite Strip Method for Thin-Walled Members with General End Boundary Conditions](#). *Journal of Engineering Mechanics*, 139(11):1566–1576.
- [5] Nguyen, V. V., Hancock, G. J., Pham, C. H. (2017). [Analyses of thin-walled sections under localised loading for general end boundary conditions – Part 1: Pre-buckling](#). *Thin-Walled Structures*, 119:956–972.
- [6] Ádány, S., Schafer, B. (2006). [Buckling mode decomposition of single-branched open cross-section members via finite strip method: Derivation](#). *Thin-Walled Structures*, 44(5):563–584.
- [7] Ádány, S., Schafer, B. (2006). [Buckling mode decomposition of single-branched open cross-section members via finite strip method: Application and examples](#). *Thin-Walled Structures*, 44(5):585–600.
- [8] Bui, H. (2009). [Buckling analysis of thin-walled sections under general loading conditions](#). *Thin-Walled Structures*, 47(6-7):730–739.
- [9] Cuong, B. H. (2012). [Elastic buckling of plates and thin-walled bars analyzed by finite strip method](#). *Journal of Science and Technology in Civil Engineering (STCE) - HUCE*, 6(1):12–23. (in Vietnamese).
- [10] Hancock, G. J., Pham, C. H. (2013). [Shear buckling of channel sections with simply supported ends using the Semi-Analytical Finite Strip Method](#). *Thin-Walled Structures*, 71:72–80.
- [11] Hancock, G. J., Pham, C. H. (2015). [Buckling analysis of thin-walled sections under localised loading using the semi-analytical finite strip method](#). *Thin-Walled Structures*, 86:35–46.
- [12] Hancock, G. J. (1978). [Local, Distortional, and Lateral Buckling of I-Beams](#). *Journal of the Structural Division*, 104(11):1787–1798.
- [13] Bui, H. C. (2012). [Semi-analytical finite strip method based on the shallow shell theory in buckling analysis of cold-formed sections](#). *Thin-Walled Structures*, 50(1):141–146.
- [14] Marguerre, K. (1950). [Knick-und Beulvorgänge](#). In *Neuere Festigkeitsprobleme des Ingenieurs*, Springer Berlin Heidelberg, 189–249.
- [15] NASA (2019). [Buckling of Thin-Walled Circular Cylinders](#). Technical report NASA/SP-8007, 2nd revision.
- [16] Seide, P., Weingarten, V. I. (1961). [On the Buckling of Circular Cylindrical Shells Under Pure Bending](#). *Journal of Applied Mechanics*, 28(1):112–116.
- [17] Silvestre, N. (2007). [Generalised beam theory to analyse the buckling behaviour of circular cylindrical shells and tubes](#). *Thin-Walled Structures*, 45(2):185–198.
- [18] Basaglia, C., Camotim, D., Silvestre, N. (2019). [GBT-based buckling analysis of steel cylindrical shells under combinations of compression and external pressure](#). *Thin-Walled Structures*, 144:106274.
- [19] Timoshenko, S. P., Gere, J. M. (1961). *Theory of elastic stability*. New York: McGraw-Hill.
- [20] Schafer, B. W. (2012). *CUFISM4.05-finite strip buckling analysis of thin-walled members*. Johns Hopkins University, Baltimore, USA.